Photoluminescence of ZnO Nanoparticles Prepared by Laser Ablation in Different Surfactant Solutions

Hiroyuki Usui, Yoshiki Shimizu, Takeshi Sasaki, and Naoto Koshizaki*

Nanoarchitectonics Research Center (NARC), National Institute of Advanced Industrial Science and Technology (AIST), Central 5, 1-1-1 Higashi, Tsukuba, Ibaraki 305-8565, Japan

Received: July 22, 2004; In Final Form: October 17, 2004

ZnO nanoparticles were prepared by laser ablation of a zinc metal plate in a liquid environment using different surfactant (cationic, anionic, amphoteric, and nonionic) solutions. The nanoparticles were obtained in deionized water and in all surfactant solutions except the anionic surfactant solution. The average particle size and the standard deviation of particle size decreased with increasing amphoteric and nonionic surfactant concentrations. With the increase of the amphoteric surfactant concentration, the intensity of the defect emission caused by oxygen vacancies of ZnO rapidly decreased, while the exciton emission intensity increased. This indicates that anionic oxygen in the amphoteric surfactant molecules effectively occupied the oxygen vacancy sites at the ZnO nanoparticle surface due to charge matching with the positively charged ZnO nanoparticles.

1. Introduction

Zinc oxide is an interesting compound semiconductor for ultraviolet (UV) LED and UV laser applications due to its wide direct band gap of 3.4 eV.[1] In addition, the exciton binding energy of 60 meV exceeds the room-temperature energy of 26 meV.[2,3] Therefore, ZnO can achieve excitonic UV emission, even at room temperature.

ZnO nanoparticles have been investigated widely as an emission material because nanocrystallization can enhance the optical and electrical properties of wide-gap semiconductors by the quantum confinement effect.[4] However, surface defects and impurity levels are easily generated during the nanoparticle formation process. The lattice defects of ZnO, such as oxygen vacancies, are known to cause a green emission.[5] Several surface treatment approaches, such as annealing in oxygen,[5] surface coating by polymeric materials,[6] embedding in a silica matrix,[7] and face-to-face annealing,[8] succeeded in suppressing the green emission intensity from ZnO nanostructures. However, these processes require multiple steps for obtaining high-intensity UV emission without green emission. Furthermore, the exciton emission intensity of CdS nanoparticles prepared by the reverse micelle method was greatly improved by promoting reactions between surface defects on CdS nanoparticles and surfactant molecules.[9] This implies that surfactant molecules play a crucial role in passivating defects on ZnO nanoparticle surfaces.

The preparation of metal nanoparticles by laser ablation in a liquid environment has recently attracted much attention.[10−18] Crystallized oxide nanoparticles can be easily obtained at room temperature by this method.[15] In addition, nanoparticles can be chemically modified using a surfactant solution in a simple one-step process. In our previous study,[16] we performed pulsed-laser ablation of a Zn metal target in an aqueous solution of anionic surfactant (sodium dodecyl sulfate, SDS), and obtained nanocomposites of β-$Zn(OH)_2$ sheets and self-assembled SDS molecule layers. The formation of nanocomposites is attributed to the charge-matching effect of imperfect zinc hydroxide sheets $Zn(OH)_x^{(2-x)+}$ with positive charge and dodecyl sulfate anions. ZnO nanoparticles were obtained when deionized water was used as the liquid medium for the laser ablation of Zn metal. However, the effect of other surfactant solutions on the product has never been explored.

In this study, we prepared ZnO nanoparticles by laser ablation in a liquid environment in different surfactant (cationic, anionic, amphoteric, and nonionic) solutions, aiming for ZnO nanostructures with strong UV emission using a simple one-step process. The influence of surfactant molecules on the morphology and photoluminescence of ZnO nanoparticles was investigated.

2. Experimental Section

A zinc metal plate (99.5%) was irradiated in the solutions by a third harmonic (355 nm) of a Nd:YAG pulse laser (Continuum, Powerlite Precision 8000) with a repetition rate of 10 Hz, pulse width of 5−7 ns, and power of 1.0 W. The laser was focused to a 1.5 mm^2 spot on the Zn target using a lens with a focal length of 250 mm. The laser fluence was estimated to be 6.7 J/cm^2. The target was fixed at the bottom of a glass vessel, which was rotated during the ablation to avoid deep ablation traces by continuous irradiation of the laser beam.

The ablation was performed in four kinds of surfactant aqueous solutions or deionized water with a volume of 10 cm^3. The cationic surfactant used was cetyltrimethylammonium bromide (CTAB), the anionic surfactant used was sodium dodecyl sulfate (SDS), the amphoteric surfactant used was lauryl dimethylaminoacetic acid betaine (LDA), and the nonionic surfactant used was octaethylene glycol monododecyl ether (OGM). The critical micelle concentration (cmc) of CTAB[19] was 9.2×10^{-4} mol/dm^3, that of SDS[20] 8.1×10^{-3} mol/dm^3, that of LDA[21] 1.8×10^{-3} mol/dm^3, and that of OGM[22] 1.1×10^{-4} mol/dm^3 at 25 °C. We also changed the concentration of the surfactant solutions from 1×10^{-4} to 1×10^{-2} mol/dm^3 for the laser ablation experiments.

Colloidal suspensions of ZnO nanoparticles were obtained by laser ablation of a Zn metal target in solutions for 1 h at room temperature. The suspensions were dropped on a copper

* To whom correspondence should be addressed. Phone: +81-29-861-6358. Fax: +81-29-861-6355. E-mail: koshizaki.naoto@aist.go.jp.

10.1021/jp046747j CCC: $30.25
Published on Web 12/10/2004

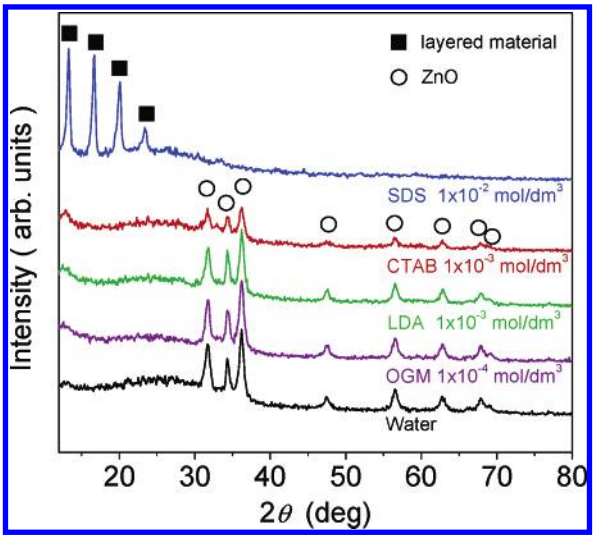

Figure 1. XRD patterns of products prepared in deionized water and different surfactant solutions around their cmc's. The layered material obtained in SDS solution is the organic/inorganic nanocomposite composed of β-$Zn(OH)_2$ sheets and dodecyl sulfate ions.[16]

mesh covered with an amorphous carbon film for observation by a field emission scanning electron microscope (Hitachi S-4800) and transmission electron microscope (JEOL JEM-2010). The sizes of nanoparticles prepared under various conditions were statistically analyzed using 100 nanoparticles in field emission scanning electron microscopy (FE-SEM) images. Precipitates of the products were repeatedly centrifuged at 50000 rpm for 30 min by an ultracentrifuge (Hitachi CS100GXL with an S100AT6 rotor), and the obtained sediments were washed with deionized water several times to remove surfactant molecules. The X-ray diffraction (XRD; Rigaku RAD-C, Cu Kα radiation) measurement and X-ray photoelectron spectroscopic (XPS; Perkin-Elmer PHI-5600ci) analysis were performed for the precipitates dried on the glass and Si substrates. The optical properties of ZnO nanoparticle-dispersed suspensions were evaluated by a UV−vis spectrophotometer (Shimadzu UV-2100PC) and a fluorophotometer (Shimadzu RF-5300PC) excited at 340 nm (3.65 eV) without a cutoff filter at room temperature.

3. Results and Discussion

Figure 1 depicts XRD patterns of the products prepared in deionized water and different surfactant solutions with concentrations near their cmc's. ZnO diffraction peaks were observed from the product prepared in water. Results clearly indicated that ablated Zn species were oxidized by H_2O during the process. In the case of all surfactant solutions except SDS solutions, the diffraction patterns of ZnO were also found and the surfactant concentration did not affect the diffraction patterns. In contrast, the products prepared in the SDS solutions exhibited a diffraction pattern from a layered organic/inorganic nanocomposite composed of β-$Zn(OH)_2$ sheets and dodecyl sulfate anions, not from ZnO, as previously reported and discussed.[16]

Figure 2 presents the optical transmittance spectra of the colloidal suspensions prepared in water and the different surfactant solutions around the cmc's. The absorption edges of ZnO were observed at 360 nm for all solutions except the SDS solution, which agrees with the results of XRD measurements. The optical band gap of ZnO nanoparticles was estimated to be about 3.36 eV from the absorption onset obtained by extrapolating the steep linear part of the transmittance spectra. This value is almost equal to the bulk band gap of ZnO

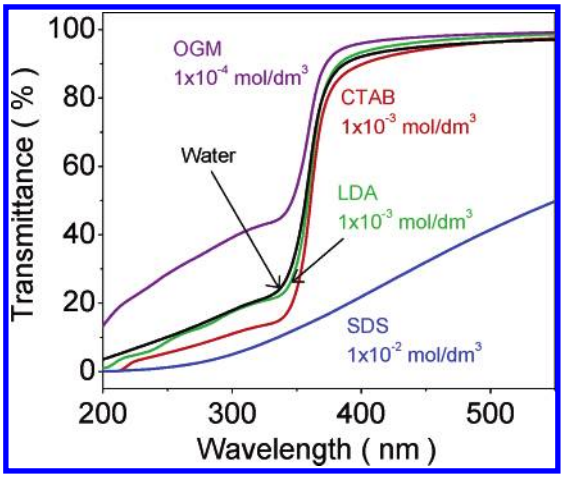

Figure 2. Transmittance spectra of colloidal suspensions prepared in water and different surfactant solutions around the cmc's.

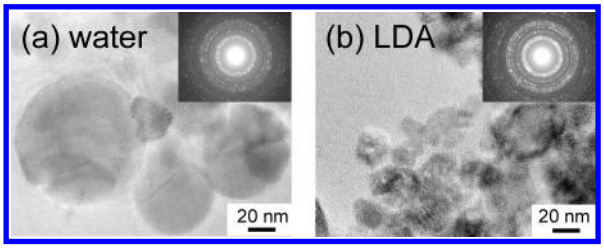

Figure 3. TEM images of ZnO nanoparticles prepared in (a) water and (b) LDA solution of 1×10^{-3} mol/dm^3 concentration. The insets depict the selected area electron diffraction patterns.

(3.4 eV). The quantum size effects of ZnO are reported to appear for particle sizes below 7 nm.[23] Therefore, the particle size of ZnO nanoparticles prepared in this study is thought to be larger than 7 nm. The layered material produced in the SDS solution was about 2 μm in diameter, leading to the low transmittance in the visible range due to light scattering. Thus, the product obtained in the SDS solution is completely different from that obtained in other surfactant solutions. Hereafter, we will focus on the nanoparticles produced in the surfactant solutions except for SDS.

Figure 3 depicts transmission electron microscopy (TEM) images of ZnO nanoparticles prepared in water and LDA solution of 1×10^{-3} mol/dm^3 concentration. Smaller ZnO nanoparticles were obtained in the LDA solution. In both cases, the lattice fringes of crystals were observed, indicating the formation of crystallized nanoparticles. The insets in Figure 3 depict the selected electron diffraction patterns of ZnO nanoparticles. The lattice spacings obtained from the diffraction rings agreed well with those of the wurtzite ZnO (JCPDS 89-1397).

Figure 4 depicts a typical FE-SEM image of ZnO nanoparticles prepared in water, and the analyzed particle size distribution with the statistical parameters in the inset. Round ZnO nanoparticles of various sizes were observed in the image. The size distribution was evidently broad and appeared to be bimodal. Figure 5 compares the size distributions of the ZnO nanoparticles prepared in the different surfactant solutions with various surfactant concentrations. The ZnO nanoparticles in the CTAB solutions are large and have a broad size distribution as in the case of water. However, ZnO nanoparticles in the LDA and OGM solutions exhibited a smaller average size and a narrow size distribution. In addition, the average size and the standard deviation decreased with increasing LDA and OGM concentrations. In particular, the average size abruptly decreased in both cases when the surfactant concentrations exceeded the cmc's. Thus, a sufficient number of LDA and OGM surfactant

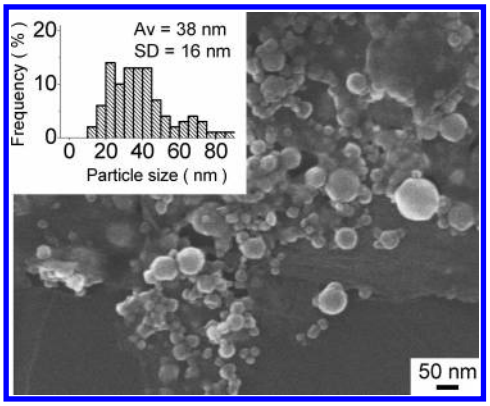

Figure 4. FE-SEM image and particle size distributions of ZnO nanoparticles prepared in deionized water. Av and SD represent the average and standard deviation of the particle size distribution.

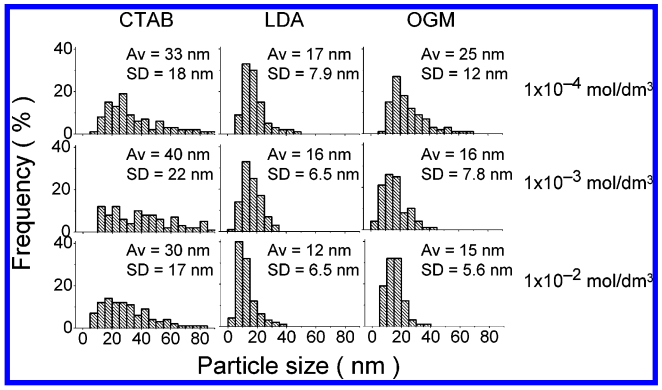

Figure 5. Particle size distributions of ZnO nanoparticles prepared in CTAB, LDA, and OGM surfactant solutions with various concentrations. Av and SD represent the average and standard deviation of the corresponding particle size distribution.

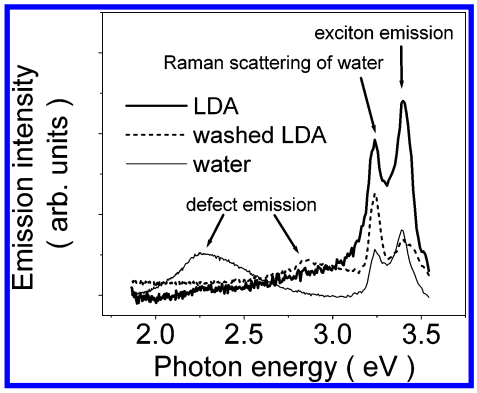

Figure 6. Photoluminescence spectra of the colloidal suspensions of ZnO nanoparticles prepared in water and LDA solution of 1×10^{-2} mol/dm^3 concentration before and after washing with deionized water.

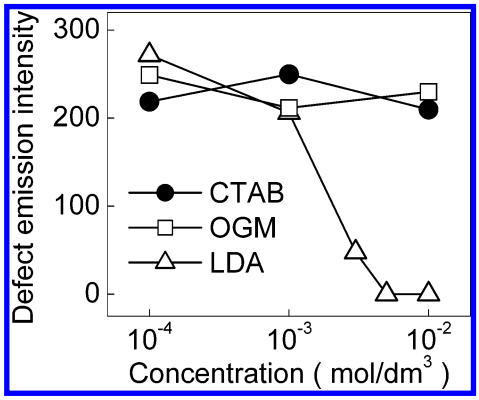

Figure 7. Surfactant concentration dependence of the defect emission intensity from colloidal suspensions of ZnO nanoparticles prepared under various surfactant conditions. The defect emission intensity was normalized by the weight loss of the target during the ablation.

molecules are expected to suppress the growth and aggregation of ZnO nanoparticles. The ZnO peaks of XRD spectra in Figure 1 have similar widths in water and all surfactant solutions except SDS, suggesting that the larger particles obtained in water and CTAB as depicted in Figure 3a were polycrystals or aggregations.

The pH was measured before and after the ablations to investigate the charge state of the ZnO nanoparticles in the solutions. The pH value tended to increase from about 7.0 to between 7.3 and 8.0, and the pH variation did not depend on the kind of solution. ZnO nanoparticles possibly have a positive electric charge in the solutions because the isoelectric point of ZnO is 9.5 in aqueous solutions.[24] The LDA molecule, $CH_3(CH_2)_{11}N^+(CH_3)_2CH_2COO^-$, has a local negative charge at the end of its hydrophilic group, while the OGM molecule, $C_{12}H_{25}(O^{\delta-}CH_2CH_2)_8OH$, also has a weak negative charge at the ether oxygen atom. Therefore, the LDA and OGM molecules surround ZnO nanoparticles due to the electric attractive force between ZnO nanoparticles and the molecules, and the formation of micelles is supposed to prevent the aggregation and growth of ZnO nanoparticles. This probably leads to smaller nanoparticle sizes in the LDA and OGM solutions.

Figure 6 depicts the emission spectra of ZnO colloidal suspensions obtained in water and the LDA solution of 1×10^{-2} mol/dm^3 concentration. Exciton emission peaks were observed at 3.40 eV for both cases. The peak observed at 3.27 eV was identified to be a Raman peak of water, since the peak was also detected even from the deionized water, and the energy difference of 3350 cm^{-1} from the excitation light corresponded well to the reported value of the Raman peak of water (3300 cm^{-1}).[25] A broad defect emission peak also appeared at 2.29 eV in the green light region for ZnO nanoparticles prepared in water. Defect emissions of yellow and green light were reported to appear at 2.15 and 2.28 eV due to lattice defects of oxygen interstitials and vacancies.[26] The defect emission of ZnO nanoparticles prepared in water is thus thought to be caused by the oxygen vacancies of ZnO. The defect emissions were observed also for CTAB and OGM solutions at the same photon energy.

The emission intensities from different surfactant solutions should be carefully compared since the amount of emitting nanoparticles in different solutions may change. Figure 7 illustrates the surfactant concentration dependence of the defect emission intensity in the visible light range normalized by the weight loss of the zinc target during ablation. In the CTAB and OGM solutions, no significant influence of the surfactant concentration on the normalized defect emission intensity was found. However, in the LDA solution, the defect emission intensity rapidly decreased above 1×10^{-3} mol/dm^3, which nearly corresponds to the cmc of LDA (1.8×10^{-3} mol/dm^3). Thus, the micelle structure formation above the cmc played a role in the effective passivation of oxygen vacancies preferentially located at the nanoparticle surface. It is quite reasonable to consider that nanoparticle cores are well crystallized due to the initial hot nanoparticle formation process by laser ablation, and that nanoparticle surfaces contain defects due to the quenching at the plasma−liquid interface. Oxygen ions in the carboxyl group of LDA surfactant molecules probably attach and passivate oxygen vacancies at the nanoparticle surfaces during the micelle formation process. The OGM molecules could

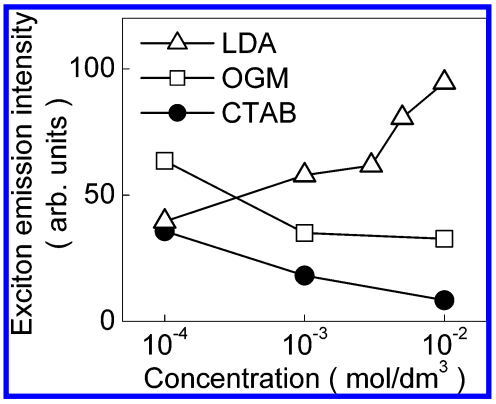

Figure 8. Surfactant concentration dependence of the exciton emission intensity from colloidal suspensions of ZnO nanoparticles prepared under various surfactant conditions. The exciton emission intensity was also normalized by the weight loss of the target during the ablation.

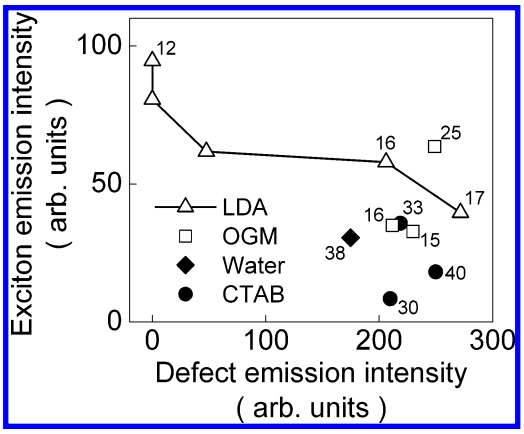

Figure 9. Relationship of the exciton emission intensity and the defect emission intensity. Numbers near the data points denote the average sizes of the nanoparticles (nm).

not sufficiently passivate the surface defect by the negative charge of the oxygen atom in the ether chain, as in the case of a CTAB molecule that is positively charged in water.

Figure 8 illustrates the surfactant concentration dependence of the normalized integral intensity of the exciton emission in the UV range. The exciton emission intensity increased concurrently with the LDA concentration, though higher concentrations of OGM and CTAB suppressed the exciton emission. ZnO nanoparticles with an average size of 12 nm prepared in LDA solution (1×10^{-2} mol/dm^3) possibly have well-crystallized cores and thin surface layers passivated by LDA molecules. In this case the contributions to exciton emission from the surface layers and from the cores are comparatively of the same order. Thus, the emission intensity nearly doubled with the LDA concentration increase as depicted in Figure 8.

Figure 9 summarizes the relationship between the exciton emission intensity and the defect emission intensity of the ZnO nanoparticles prepared under various surfactant conditions. The ZnO nanoparticles prepared in the LDA solutions revealed that the exciton emission intensity increased with decreasing defect emission intensity. Defect emission from the nanoparticles prepared in OGM could not be passivated by the small local charge of the OGM molecule, though the nanoparticles were slightly larger than those in LDA and were single-crystalline. This nanoparticle formation process is possibly assisted by the micelle formation of surfactant. For CTAB, surface defects could not be passivated by the positive charge of the ionized CTAB molecule. Furthermore, the particles were relatively large and presumably polycrystalline, since micelle formation did not effectively hinder aggregation as in water without any surfactant. Defects might be included at the grain boundary of large polycrystalline nanoparticles and also act as recombination centers, leading to small exciton emission.

The passivation stability of the green defect emission by the LDA surfactant was also examined. The produced ZnO nanoparticles in LDA solution were repeatedly ultracentrifuged, dispersed in deionized water, and ultrasonically separated several times to remove as many LDA molecules as possible. The photoluminescence spectrum of the colloidal suspension prepared in LDA (1×10^{-2} mol/dm^3) after the washing process is shown as a broken line in Figure 5. Another defect emission peak appeared at 2.97 eV, which might be attributed to lattice defects of zinc interstitials[27] or other impurities from LDA molecules, generated during the washing process. However, the defect emission peak of oxygen vacancies at 2.29 eV did not emerge, and the LDA molecules were still attached on the ZnO nanoparticle surface according to the observation of the nitrogen photoelectron peak (N1s) from the LDA molecule by XPS analysis. The green defect emission of ZnO nanoparticles was thus effectively passivated by the LDA molecules strongly attached on the oxygen vacancy sites of the ZnO nanoparticle surface.

4. Summary

ZnO nanoparticles were prepared by laser ablation in liquid environments in different surfactant (cationic, anionic, amphoteric, and nonionic) solutions, aiming for strong UV emission without green luminescence, by a simple one-step process. We investigated the influence of surfactant molecules and their concentrations on the morphology and photoluminescence of ZnO nanoparticles. ZnO nanoparticles were obtained in deionized water and all surfactant solutions except the anionic surfactant solutions. In the amphoteric and nonionic surfactant solutions, the average and the standard deviation of nanoparticle size decreased with the surfactant concentrations, and this decrease was prominent when the surfactant concentrations exceeded the cmc's. With the concentration increase of the amphoteric surfactant LDA, the green defect emission intensity caused by oxygen defects of ZnO decreased and the exciton UV emission increased. The results suggest that oxygen in the carboxyl group of the amphoteric surfactant molecule effectively occupied the oxygen defects at the surface of ZnO nanoparticles because the amphoteric surfactant molecules were attracted by positively charged ZnO nanoparticles. This method is expected to be very useful for passivating oxygen defects and for other nanoparticle surface modification by a simple one step process.

Acknowledgment. This study was partially supported by Industrial Technology Research Grant Program '04 from the New Energy and Industrial Technology Development Organization (NEDO) of Japan.

References and Notes

(1) Ozerov, I.; Arab, M.; Safarov, V. I.; Marine, W.; Giorgio, S.; Sentis, M.; Nanai, L. *Appl. Surf. Sci.* **2004**, *226*, 242.

(2) Kawasaki, M.; Ohtomo, A.; Ohkubo, I.; Koinuma, H.; Tang, Z. K.; Yu, P.; Wong, G. K. L.; Zhang B. P.; Segawa, Y. *Mater. Sci. Eng., B* **1998**, *56*, 239.

(3) Ohtomo, A.; Kawasaki, M.; Sakurai, Y.; Yoshida, Y.; Koinuma, H.; Yu, P.; Tang, Z. K.; Wong, G. K. L.; Segawa, Y. *Mater. Sci. Eng., B* **1998**, *54*, 24.

(4) Wang, Y.; Herron, N. *J. Phys. Chem.* **1991**, *95*, 525.

(5) Kang, J. S.; Kang, H. S.; Pang, S. S.; Shim, E. S.; Lee, S. Y. *Thin Solid Films* **2003**, *443*, 5.

(6) Yang, C. L.; Wang, J. N.; Ge, W. K.; Guo, L.; Yang, S. H.; Shen, D. Z. *J. Appl. Phys.* **2001**, *90*, 4489.

(7) Chakrabarti, S.; Das, D.; Ganguli, D.; Chaudhuri, S. *Thin Solid Films* **2003**, *441*, 228.
(8) Wang, Y. G.; Lau, S. P.; Zhang, X. H.; Hng, H. H.; Lee, H. W.; Yu, S. F.; Tay, B. K. *J. Cryst. Growth* **2003**, *259*, 335.
(9) Zhang, J.; Sun, L.; Liao, C.; Yan, C. *Solid State Commun.* **2002**, *124*, 45.
(10) Simakin, A. V.; Voronov, V. V.; Shafeev, G. A.; Brayner, R.; Bozon-Verduraz, F. *Chem. Phys. Lett.* **2001**, *348*, 182.
(11) Mafuné, F.; Kondow, T. *Chem. Phys. Lett.* **2004**, *383*, 343.
(12) Mafuné, F.; Kondow, T. *Chem. Phys. Lett.* **2003**, *372*, 199.
(13) Chen, Y. H.; Yeh, C. S. *Colloids Surf., A* **2002**, *197*, 133.
(14) Anikin, K. V.; Melnik, N. N.; Simakin, A. V.; Shafeev, G. A.; Voronov, V. V.; Vitukhnovsky, A. G. *Chem. Phys. Lett.* **2002**, *366*, 357.
(15) Liang, C. H.; Shimizu, Y.; Sasaki, T.; Koshizaki, N. *J. Phys. Chem. B* **2003**, *107*, 9220.
(16) Liang, C. H.; Shimizu, Y.; Sasaki, T.; Koshizaki, N. *Chem. Mater.* **2004**, *16*, 963.
(17) Liang, C. H.; Shimizu, Y.; Sasaki, T.; Koshizaki, N. *Chem. Phys. Lett.* **2004**, *389*, 58.
(18) Huang, C.-C.; Yeh, C.-S.; Ho, C.-J. *J. Phys. Chem. B* **2004**, *108*, 4940.
(19) Imae, T.; Kamiya, R.; Ikeda, S. *J. Colloid Interface Sci.* **1985**, *108*, 215.
(20) Mysels, K. J. *Langmuir* **1986**, *2*, 423.
(21) Beckett, A. H.; Woodward, R. I. *J. Pharm. Pharmacol.* **1963**, *15*, 422.
(22) Becher, P. *J. Phys. Chem.* **1959**, *63*, 1675.
(23) Koch, U.; Fojtik, A.; Weller, H.; Henglein, A. *Chem. Phys. Lett.* **1985**, *122*, 507.
(24) Degen, A.; Kosec, M. *J. Eur. Ceram. Soc.* **2000**, *20*, 667.
(25) Vallee, P.; Lafait J.; Ghomi M.; Jouanne M.; Morhange J. *J. Mol. Struct.* **2003**, *651*, 371.
(26) Ong, H. C.; Du, G. T. *J. Cryst. Growth* **2004**, *265*, 471.
(27) Fang, Z.; Wang, Y.; Xu, D.; Tan, Y.; Liu, X. *Opt. Mater.* **2004**, *26*, 239.